EARTHQUAKE ENGINEERING AND STRUCTURAL DYNAMICS, VOL. 18, 617 631 (1989)

ATTENUATION OF SEISMIC INTENSITY IN ALBANIA AND YUGOSLAVIA

M. D. TRIFUNAC AND M. I. TODOROVSKA

Department of Civil Engineering, University of Southern California, Los Angeles, CA 90089-1114, USA

SUMMARY

Average and standard deviations of hypocentral distances to selected isoseisms are presented for Albania and Yugoslavia. The results apply for the Medvedev–Karnik–Sponheuer (MKS) intensity, provided that all data are corrected to a unified MKS equivalent intensity as defined by Shebalin *et al.*[19] The results should be useful in general macroseismic studies in these two countries, but are essential for the development of microzonation maps when the seismicity is described in terms of the locally available intensity catalogues.

The observed attenuation of the intensities versus the hypocentral distance is similar to the attenuation of the Modified Mercalli Intensity (MMI) in the western United States of America. This finding should facilitate the use of other empirical scaling relations, developed in California, for various predictions of the characteristics of strong earthquake shaking in Albania and Yugoslavia.

INTRODUCTION

The subject of the intensity attenuation with distance has been studied extensively, but most investigators have focused only on the description of the mean trends and little or no attention has been paid to the scatter of observed data, although it is recognized that this scatter is very important (e.g. Gupta and Nuttli,[6] Howell and Schultz,[8] Bollinger[3]). With the development of the Uniform Risk Spectrum (URS) technique[2,11] and its application in the new microzonation method,[10,23] the need for the probabilistic description of the attenuation of intensity with distance grew and the results of several studies, in different geologic and tectonic settings, are now available.[1,5] A description of the attenuation of intensities with a single curve through the mean trend neglects the scatter in the data and is therefore incomplete.

The Uniform Risk Spectrum (URS) method offers a systematic procedure, which incorporates, in a balanced way, (i) the seismicity of various sources in the area surrounding the site, (ii) the geometrical distribution and the shape of earthquake sources, (iii) attenuation along different geological paths and (iv) the local soil and geologic conditions, for determination of the distribution functions of the levels of strong ground shaking. This method has been developed first for the computation of the site specific design spectra of important structures[27–29] but it can be used also for detailed mapping of seismic risk.[10,12,23] To use this microzonation method it is necessary first to define the seismicity in the area using the data on historic seismicity (usually available only in terms of catalogues containing non-instrumental data, and in terms of the seismic intensity scales). Even when such data are readily available, it is seldom in the form that it can be used directly, because the computer programs for computation of the Uniform Risk Spectra, URS[11] require $P\{I<I_1|I_0, \Delta\}$, that is the probability that the intensity I will take values less than I_1 at a site at distance Δ from the source and where the epicentral intensity is I_0. The hypocentral distance $\Delta=(R^2+H^2)^{1/2}$, where R is the epicentral distance and H is the depth of focus, and I_1 is some selected intensity such that $I_1 \leqslant I_0$. Anderson[1] has shown how $P\{I<I_1|I_0, \Delta\}$ can be developed from the maps of contoured isoseismals in the United States and Gupta and Trifunac[5] have applied this method to the Indian subcontinent. The purpose of this work is to present similar analyses for Albania and Yugoslavia in south-eastern Europe, and thus to enable the use of the URS method for selection of site specific design spectra and for the development of micro and macrozonation maps there.

0098–8847/89/050617–15$07.50

Received 14 June 1988

To carry out the seismic risk calculations it is also necessary to have the relationships between the local intensity scales and the actually recorded amplitudes and duration of strong earthquake ground motion (e.g. Trifunac and Lee[25, 26]). At present there are enough recorded data in the western United States and in Japan to develop such empirical correlations. In other parts of the world, including the Balkan countries (Figure 1), the data available at this time are not adequate to determine such correlations independently. Though such analyses are beyond the scope of this work, it is important to note this here, because the development of $P\{I < I_1 | I_0, \Delta\}$ functions is necessary for the implementation of seismic risk and microzonation calculations, but not sufficient, unless it is carried out together with the development of the direct empirical scaling of

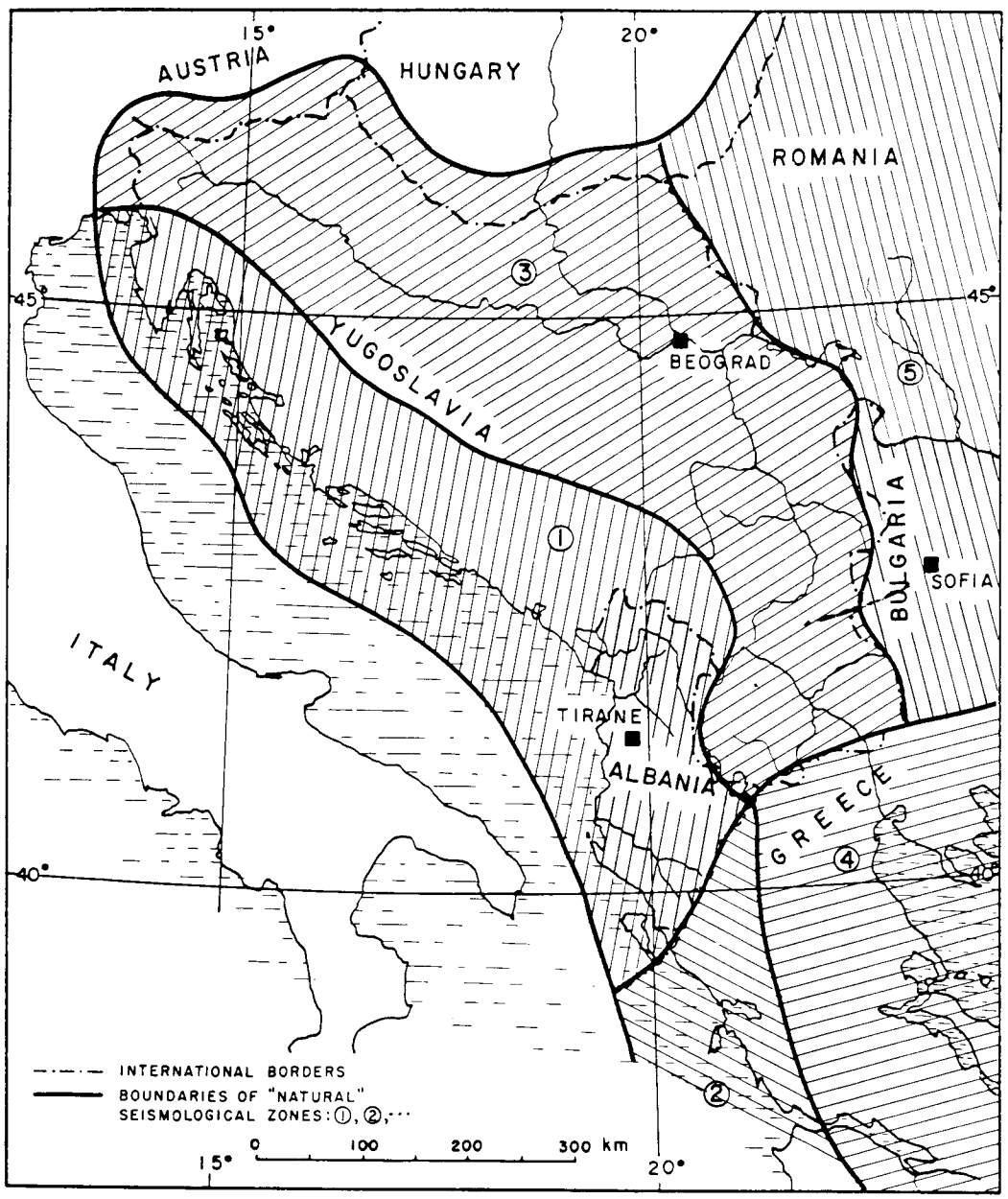

Figure 1. Boundaries of the chosen 'natural' seismological zones (1 to 5) for Albania, Yugoslavia and neighbouring countries

intensities with the data actually recorded in the area. With the recent completion of the strong motion data base for Yugoslavia[9] it will become possible to initiate the work on this task in the near future.

DESCRIPTION OF DATA

The data used in this work (Figure 2) come from the *Catalogue of Earthquakes* edited by Shebalin, Kárnik and Hadžievski.[19] This report presents data on isoseismals for the entire Balkan region and the western part of Turkey with $I_0 \geq$ VIII for the years prior to 1800, $I_0 \geq$ VII for the period 1801 to 1970 and $I_0 >$ VI for the

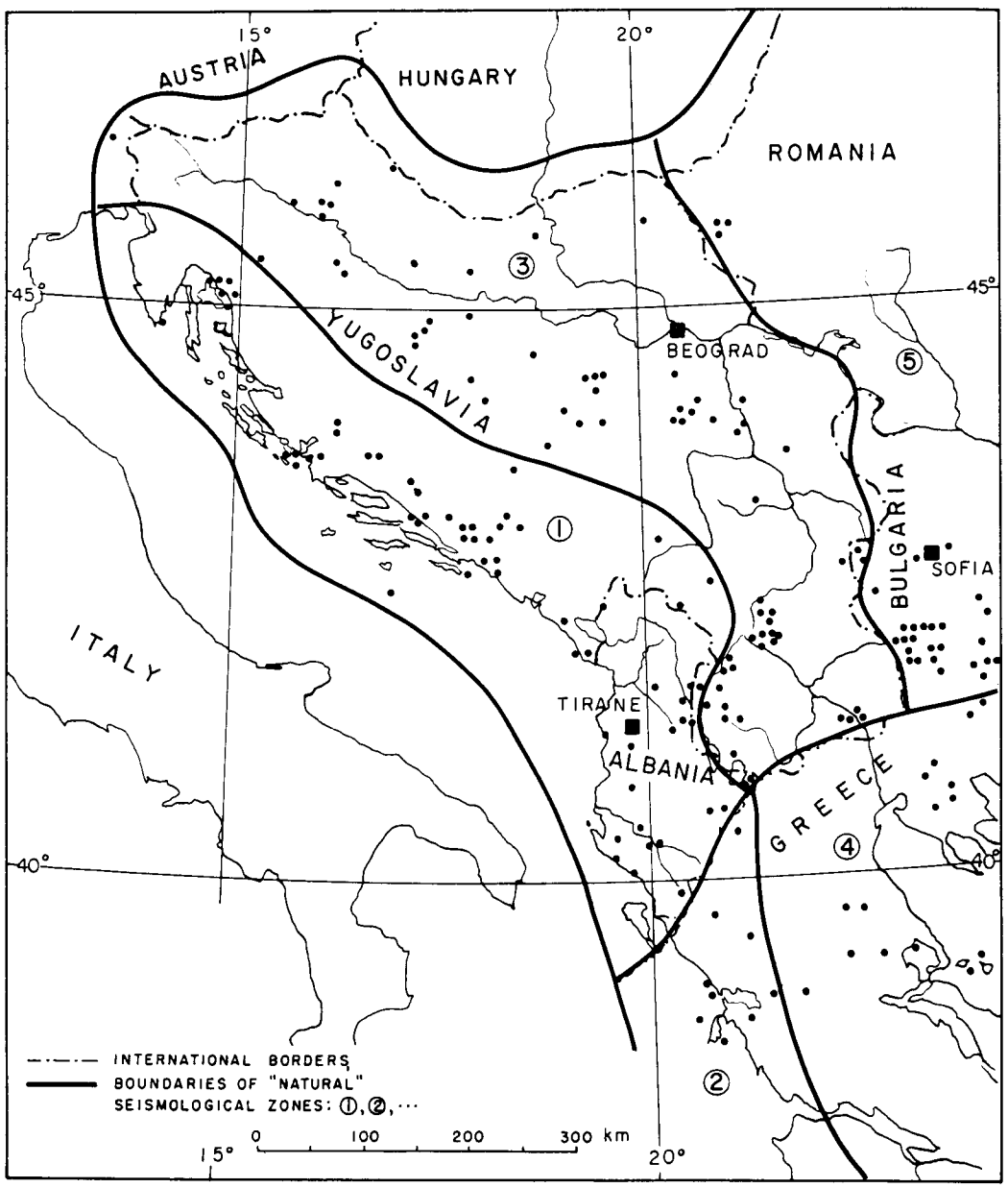

Figure 2. Epicentres of 143 earthquakes selected for this study

period 1901 to 1970. For the period 1901 to 1970, 454 isoseismal maps have been presented and chosen for publication. Of these 143 were sufficiently complete for the requirements of this analysis and for the area studied in this paper. The total number of isoseismals presented for the Balkan project by Shebalin *et al.*[19] does not represent the distribution or the actual number of earthquakes in this area. This resulted from non-uniform characteristics of different national catalogues and their various levels of completeness. While the different methods used in these catalogues offered certain advantages in their respective countries, it was necessary for the investigators of the Balkan project to choose some unified method of presentation and to show the 'complete macroseismic information in a homogeneous form'. This impressive work on revision, completion, generalization and final drawing of isoseismal maps has been carried out by N.V. Shebalin and I. Todorov (Shebalin *et al.*[19]). It is only thanks to this effort that our present analysis is possible.

Various seismic intensity scales have been in use in the Balkan region during different periods, and different interpretations of similar scales in the neighbouring countries are portrayed by the maps which are presented in this *Catalogue of Earthquakes*. Their final relationship is presented in Figure 3. Some of these scales were used differently during different periods. For example, the scales used by Prof. Mihailović changed with time and are labelled as: RF-M (used before 1912–1914), FM-M (used between 1912–1913 and 1922–1923) and MCS-M (used from 1922 and 1923 to 1945–1950).

The detailed review of the mutual relationships of different scales and the empirical relationships for their conversion to the standard MKS scale have been presented by Shebalin.[18] Since one of the aims of Shebalin *et al.*[19] has been to 'homogenize' and to 'unify' the method of presentation of isoseismal maps for the whole Balkan region, a set of 'generalized' isoseismals which neglect the 'local effects on the earth surface have been drawn'. These generalized and smoothed isoseismals were chosen by us as the data base for this project.

In their analysis on the attenuation of intensities with epicentral distance Shebalin *et al.*[19] considered both 'technical' and 'natural' boundaries between different geographical zones. The 'technical' boundaries were considered because of the possible differences in national practices in the determination of the relevant earthquake parameters. The 'natural' seismological zones were chosen on the basis of different tectonic environment and to study the effects of this geologic environment on attenuation. In this work we have adopted the same 'natural' zones as proposed by Shebalin *et al.*[19] For the portion of the Balkan region which is studied in this paper these 'natural' seismological zones are (Figure 1):

1. Outer area of the Dinarides and the Illyrides,
2. From Hellenides to Crete and Rodos,
3. Inner part of the Balkan Peninsula west of Romania and Bulgaria and north of Greece,
4. Central and eastern Greece and the Aegean Sea,
5. Inner part of the Balkan Peninsula covering most of Romania and Bulgaria.

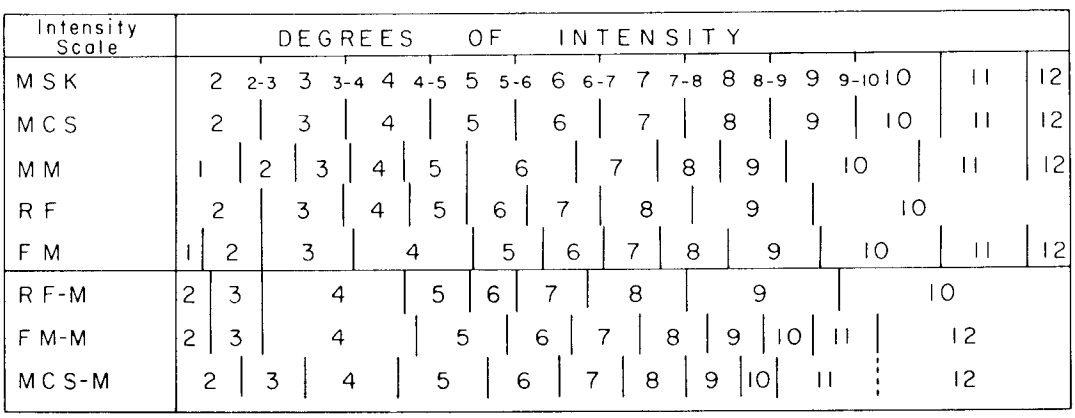

Figure 3. Correlation of seismic intensity scales used in the Balkan countries (after Shebalin[18])

Figure 2 shows the epicentres of the 143 earthquakes in regions 1 and 3 which were analysed in this paper.

METHODS OF ANALYSIS

Figure 4 (redrawn from Anderson[1]) shows sixteen radii drawn from the epicentre. The distances to each isoseismal in the direction of these radii (e.g. R_6) were measured, tabulated and stored into computer files. When an isoseism was drawn over water or with a broken line, it was not included in the data base (e.g. R_5 on line 16). After reading all the maps in this manner the data were grouped according to the maximum intensity, I_0, and from that point on the analysis followed the same steps as described in Anderson.[1]

Figures 5(a) and 5(b), corresponding to regions 1 and 3 respectively, present the distribution of the available data with respect to the focal depth and the hypocentral distances $\Delta_i=(R_i^2+H^2)^{1/2}$, where R_i represent the radii (or epicentral distances) for a given isoseism and H is the focal depth of the corresponding earthquake. Bottom portions of Figures 5 show histograms of the number of the available distances, Δ_i, for intensities $I=I_0$, $I=I_0-1,\ldots,$ and $I=I_0-5$, plotted versus $\log_{10}\Delta$. The number of the available data for regions 1 and 3 is 65 and 78 respectively [Tables I(a) and I(b)].

All the distances, Δ_i, for the I_1 isoseismals corresponding to earthquakes with epicentral intensity I_0, $(I_1 \leqslant I_0)$, were grouped in increasing order forming the ordered set $\Delta_1 \leqslant \Delta_2 \leqslant \ldots \leqslant \Delta_i \leqslant \ldots \leqslant \Delta_{N_{I_0,I_1}}$. Here N_{I_0,I_1} is the number of the available distances for the isoseismal I_1 corresponding to earthquakes with epicentral intensity I_0. The probability

$$P\{I<I_1|I_0,\Delta\}=P_{I_0,I_1}(\Delta)$$

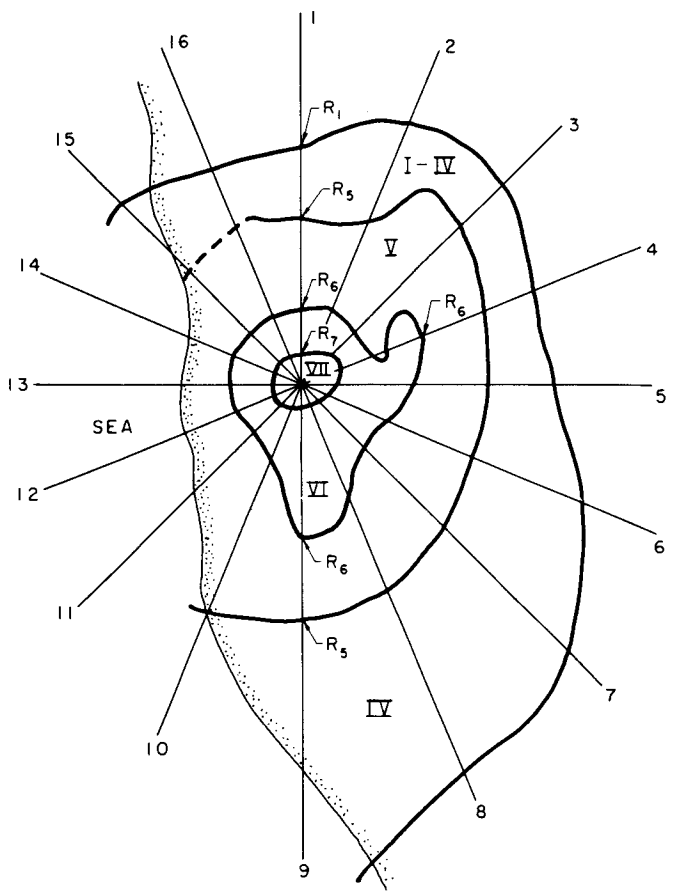

Figure 4. Example of isoseismal map showing the convention used to measure 16 radii to I_1

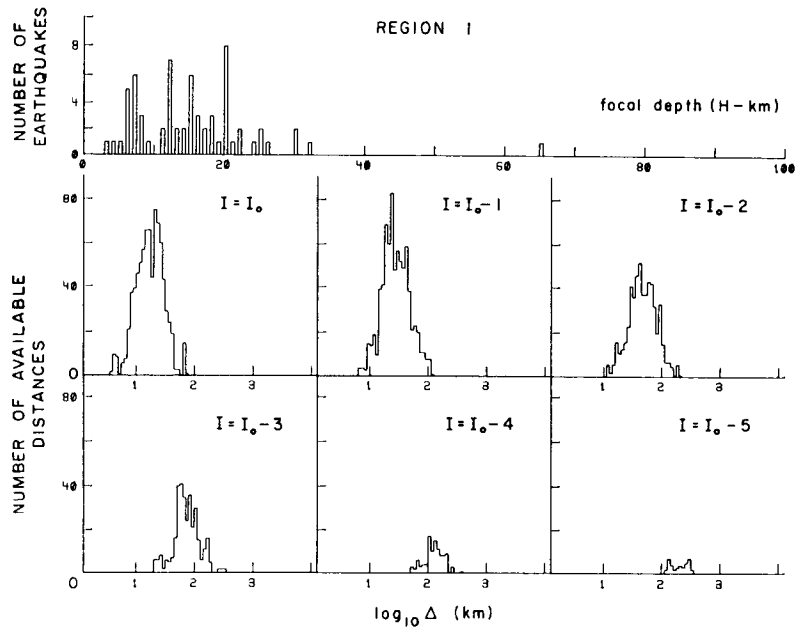

Figure 5(a). Histogram showing the distribution of earthquakes with respect to hypocentral depth, H, for region 1 (top figure). Histograms of the distribution of $\log_{10}\Delta$, where Δ is hypocentral distance in kilometres, to the isoseismals of intensity $I=I_0$, $I=I_0-1$, ..., $I=I_0-5$ in region 1

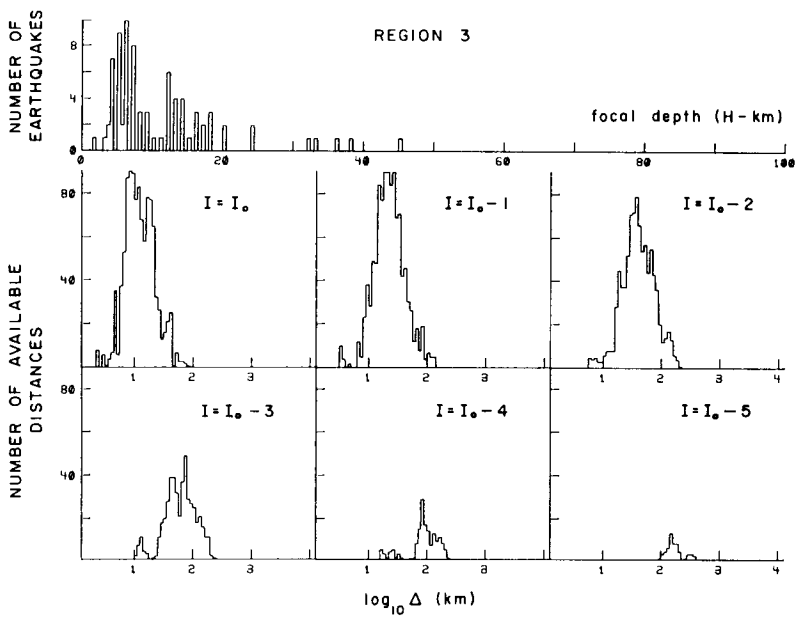

Figure 5(b). Histogram showing the distribution of earthquakes with respect to hypocentral depth, H, for region 3 (top figure). Histograms of the distribution of $\log_{10}\Delta$, where Δ is hypocentral distance in kilometres, to the isoseismals of intensity $I=I_0$, $I=I_0-1$, ..., $I=I_0-5$ in region 3

where $P_{I_0,I_1}(\Delta)$ is the cumulative distribution function for the hypocentral distances to the I_1 isoseismal when the epicentral intensity is I_0. $P_{I_0,I_1}(\Delta)$ can be approximated by the following expression:

$$P_{I_0,I_1}(\Delta)=\frac{i}{N_{I_0,I_1}}, \quad \Delta_i \leqslant \Delta < \Delta_{i+1} \tag{1}$$

Table I(a). Average and standard deviation of the logarithm of the hypocentral distance in kilometres to isoseism enclosing the area with $I \geqslant I_1$

REGION 1

EPICENTRAL INTENSITY, I_0		INTENSITY I_1							
		3	4	5	6	7	8	9	10
3·0									
3·5									
4·0									
4·5									
5·0	7		5 38	7 90					
			1·805	1·572					
			0·130	0·118					
5·5	1		1 6	1 9					
			1·696	1·457					
			0·051	0·039					
6·0	17	10 59	13 119	17 201	14 189				
		2·010	1·787	1·517	1·231				
		0·156	0·231	0·173	0·192				
6·5	5	1 8	5 29	5 51	5 80				
		2·220	1·889	1·645	1·320				
		0·029	0·092	0·218	0·180				
7·0	12	2 6	8 85	10 119	11 135	11 135			
		2·104	1·803	1·640	1·380	1·172			
		0·064	0·196	0·172	0·196	0·184			
7·5	3	2 10	1 3	3 29	3 45	3 48			
		2·149	2·155	1·768	1·492	1·243			
		0·154	0·047	0·190	0·193	0·161			
8·0	8	3 10	5 43	8 81	8 92	8 114	6 91		
		2·282	2·138	1·852	1·597	1·357	1·117		
		0·188	0·114	0·132	0·212	0·157	0·107		
8·5	2				2 17		2 32		
					1·647		1·138		
					0·159		0·265		
9·0	10	1 5	5 29	5 39	6 73	7 93	8 112	6 87	
		2·394	2·309	2·041	1·796	1·541	1·302	1·171	
		0·082	0·131	0·189	0·101	0·104	0·083	0·060	
9·5									
10·0									
	65								

The Gaussian curve $\hat{P}_{I_0,I_1}(\Delta)$ to approximate the distribution (1) is of the form

$$\hat{P}_{I_0,I_1}(\Delta)=\frac{1}{\sigma_{I_0,I_1}}\sqrt{\frac{1}{2\pi}}\int_{-\infty}^{\log_{10}\Delta}\exp\left[-\frac{1}{2}\left(\frac{\mu_{I_0,I_1}-x}{\sigma_{I_0,I_1}}\right)^2\right]dx \tag{2}$$

where μ_{I_0,I_1} and σ_{I_0,I_1} are the mean and the standard deviation of the data in the ordered set, that can be found by a least squares procedure. Finally, the maximum difference between the observed distribution function and

Table I(b). Average and standard deviation of the logarithm of the hypocentral distance in kilometres to isoseism enclosing the area with $I \geq I_1$

REGION 3

EPICENTRAL INTENSITY, I_0		INTENSITY I_1							
		3	4	5	6	7	8	9	10
3·0									
3·5									
4·0									
4·5									
5·0									
5·5									
6·0	27	9 55 1·925 0·253	21 188 1·710 0·169	25 318 1·379 0·177	25 355 1·077 0·182				
6·5	5		3 26 1·817 0·228	5 71 1·418 0·236	5 78 1·067 0·208				
7·0	29		18 214 1·780 0·220	26 362 1·531 0·204	26 363 1·275 0·196	25 359 0·972 0·167			
7·5	3	2 6 2·125 0·039	2 18 1·883 0·053	3 41 1·540 0·076	3 44 1·285 0·062	3 48 1·041 0·127			
8·0	7		7 45 2·009 0·150	7 73 1·794 0·195	7 98 1·445 0·258	7 93 1·212 0·228	4 56 1·089 0·224		
8·5	3	1 2 2·346 0·001	2 8 2·227 0·029	3 29 2·058 0·105	3 46 1·873 0·128	3 48 1·591 0·100	3 42 1·332 0·057		
9·0	3		3 34 2·268 0·121	3 42 2·006 0·090	3 48 1·773 0·200	3 48 1·577 0·188	3 44 1·327 0·104	2 23 1·121 0·018	
9·5									
10·0	1		1 5 2·378 0·036	1 14 2·157 0·090	1 15 1·890 0·048	1 16 1·677 0·108	1 16 1·512 0·118	1 15 1·326 0·049	1 13 1·222 0·010
	78								

the Gaussian approximation of the same function, ε_{I_0,I_1}, can be found as

$$\varepsilon_{I_0,I_1} = \max_i \{|\hat{P}_{I_0,I_1}(\Delta_i) - P_{I_0,I_1}(\Delta_i)|\}$$

Then, this maximum difference is compared with $\varepsilon^{KS}_{I_0,I_1}$, the Kolmogorov–Smirnov critical value for the 95 per cent confidence level. If $\varepsilon_{I_0,I_1} > \varepsilon^{KS}_{I_0,I_1}$, it means that at the 95 per cent confidence level the measured data are not members of the assumed distribution $\hat{P}_{I_0,I_1}(\Delta)$.[7] Figures 6(a) and 6(b) illustrate $P_{I_0,I_1}(\Delta)$ and $\hat{P}_{I_0,I_1}(\Delta)$ for region 1 and region 3 earthquakes with $I_0 =$ VII and VIII and $I_1 =$ IV, V, VI, VII and VIII. In the calculations those values of I_0 and I_1 were considered which were represented by 5 or more radii. In addition, Figures 6(a)

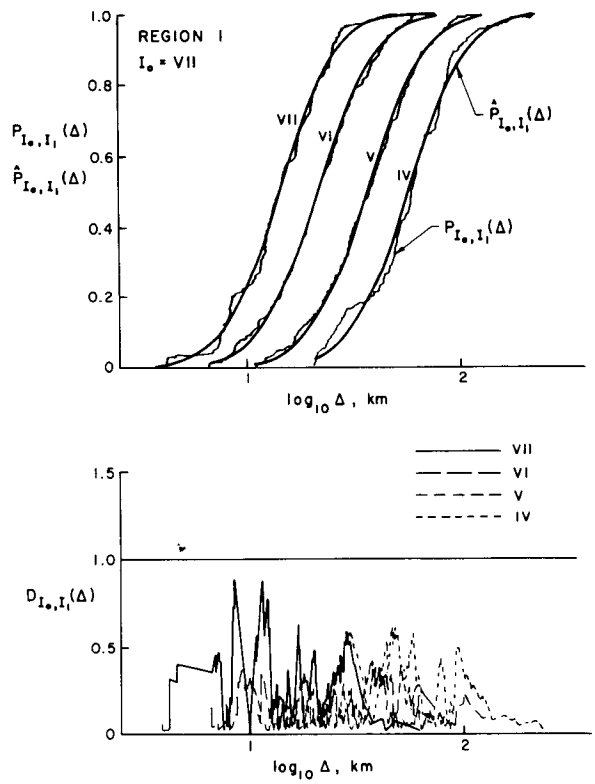

Figure 6(a). Top: Empirical distribution functions for region 1 with $I_0 = \text{VII}$ versus $\log_{10}\Delta$ (hypocentral distance). The staircase function represents $P_{I_0,I_1}(\Delta)$ determined directly from the data for $I_1 = \text{VII}$, VI, V and IV. The smooth curve is the Gaussian curve $\hat{P}_{I_0,I_1}(\Delta)$, defined in equation (2). Bottom: Error = D (hypocentral distance), shows the difference between the Gaussian and empirical distributions normalized to the Kolmogorov–Smirnov critical (95 per cent confidence) value for the number of data in this set

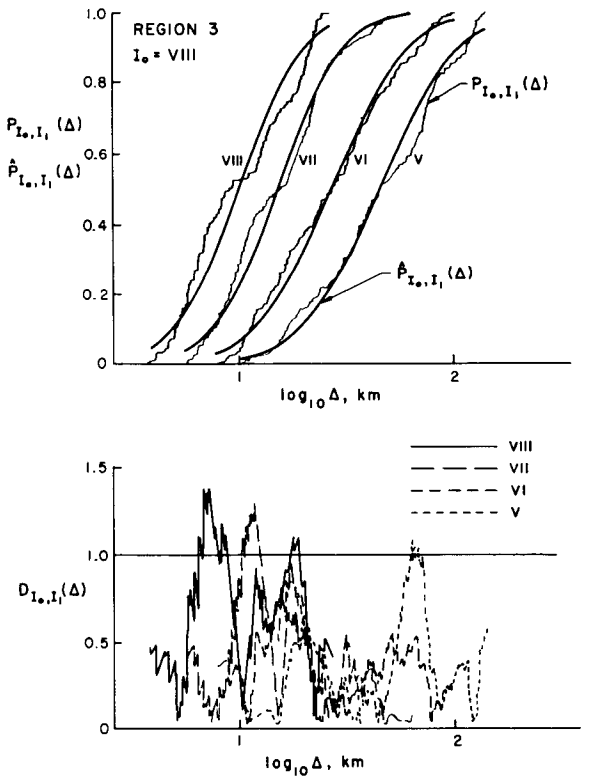

Figure 6(b). Top: Empirical distribution functions for region 3 with $I_0 = \text{VIII}$ versus $\log_{10}\Delta$ (hypocentral distance). The staircase function represents $P_{I_0,I_1}(\Delta)$ determined directly from the data for $I_1 = \text{VIII}$, VII, VI and V. The smooth curve is the Gaussian curve $\hat{P}_{I_0,I_1}(\Delta)$, defined in equation (2). Bottom: Error = D (hypocentral distance), shows the difference between the Gaussian and empirical distributions normalized to the Kolmogorov–Smirnov critical (95 per cent confidence) value for the number of data in this set

and 6(b) show the 'error' functions $D_{I_0,I_1}(\Delta)$ defined by

$$D_{I_0,I_1}(\Delta) = \max_i \{|\hat{P}_{I_0,I_1}(\Delta_i) - P_{I_0,I_1}(\Delta_i)|/\varepsilon^{KS}_{I_0,I_1}\}$$

The error functions give the normalized difference between the distribution of distances implied by the data and the Gaussian approximation of this data. Since $P_{I_0,I_1}(\Delta)$ is multiple valued for each distance $\Delta = \Delta_i$ [equation (1)], the value of $P_{I_0,I_1}(\Delta_i)$ which leads to the largest value of $D_{I_0,I_1}(\Delta)$ is used to compute $D_{I_0,I_1}(\Delta)$ at these points. Because $\varepsilon^{KS}_{I_0,I_1}$ is selected to normalize the difference between $P_{I_0,I_1}(\Delta)$ and $\hat{P}_{I_0,I_1}(\Delta)$, whenever $D_{I_0,I_1}(\Delta) > 1{\cdot}0$ at some value of Δ, $\hat{P}_{I_0,I_1}(\Delta)$ is rejected by the Kolmogorov–Smirnov test, at the 95 per cent confidence level, as an acceptable model for $P_{I_0,I_1}(\Delta)$. By examining $D_{I_0,I_1}(\Delta)$, then, it is possible to tell how well the model $\hat{P}_{I_0,I_1}(\Delta)$ approximates $P_{I_0,I_1}(\Delta)$. For example, in Figure 6(b) the 'error' function $D_{I_0,I_1}(\Delta)$ is larger than 1 for $I_1 = \text{VIII}$, VII and V, for distances Δ around 6, 18, 11 and 63 km respectively. In Figure 6(a), $D_{I_0,I_1}(\Delta) < 1$ for all R. In this work, however, we will accept the approximate Gaussian distribution model given by equation (2), even when some $D_{I_0,I_1}(\Delta)$ functions exceed 1 locally, because the overall amplitudes of $D_{I_0,I_1}(\Delta)$ are much less than 1, because many of the peaks of $D_{I_0,I_1}(\Delta)$ which exceed 1 at 95 per cent confidence would become acceptable at 90 per cent confidence level, and because many discrepancies between the data and the model result from incomplete data rather than from some obvious physical reason for rejecting the

Gaussian nature of the assumed distribution. We found an excellent fit of the model in equation (2) and $D_{I_0,I_1}(\Delta)<1$ in most cases for both regions.

Tables I(a) and I(b) present the computed μ_{I_0,I_1} and σ_{I_0,I_1} for both regions 1 and 3 as calculated from the available data. I_0 is shown in the first vertical column, while I_1 increases along horizontal rows starting with the third column. For example, in Table I(a), 1·796 represents the logarithm of the average distance to $I_1=$ VI for an earthquake with epicentral intensity $I_0=$ IX. The corresponding $\sigma_{\text{IX,VI}}=0{\cdot}101$. The second column in Tables I(a) and I(b) shows the total number of earthquakes (isoseismal maps) contributing to the data summarized in that row of tables. For each I_0 and for each μ_{I_0,I_1} and σ_{I_0,I_1} the total number of contributing earthquakes (e.g. 6 for $I_0=$ IX and $I_1=$ VI) and the total number of contributing distances to isoseismals (e.g. 73 for $I_0=$ IX and $I_1=$ VI) are also presented.

ATTENUATION EQUATIONS

One approach to modelling the mean values, μ_{I_0,I_1} is to use an extension of the method used in Nuttli[13,14] and Gupta and Nuttli.[6] One reason for this choice arises from the expected uses in engineering applications and in risk analyses, where log (amplitude) of ground motion is often assumed to be proportional to a numerical value equal to the Roman numeral which represents a level of MKS intensity. To be consistent with this usage, the model to describe the attenuation of MKS intensity should assume that the intensity is proportional to the log (amplitude) of ground motion. (This assumption is usually not contradicted by the data[20, 24]). Furthermore, by making such assumptions, it can be shown that the attenuation of intensity can be described by the attenuation of seismic wave amplitudes.

The equation

$$\left(\frac{A}{T}\right)(D)=K(D)^{-1/2}(\sin D)^{-1/2}\,\mathrm{e}^{-\gamma D} \tag{3}$$

describes the amplitude of the particle velocity in a dispersed surface wave which is not travelling in the Airy phase.[14] A is the displacement amplitude of a wave with period T at an epicentral distance D (radians), constant K is related to the amplitude at the source and γ is the coefficient of anelastic attenuation. For distances greater than 50 km, equation (3) closely approximates the empirical attenuation curve developed by Richter[16] for the local magnitude scale in southern California when $\gamma=0{\cdot}60$/deg. Equation (3) also describes the attenuation of $(A/T)_{\max}$ for the vertical component of Rayleigh waves of 3–12 sec period from earthquakes in the central United States when $\gamma=0{\cdot}10$/deg; for the vertical component of 1 sec period Lg waves in the same region, and for $\gamma=0{\cdot}07$/deg.

Nuttli[13] shows that a selected intensity corresponds to similar values of (A/T) in the eastern and the western United States. This suggests that Modified Mercalli (and MKS) Intensity can be correlated with (A/T), and Gupta and Nuttli[6] suggest a relationship of the form

$$I_0-I(D)=a+b\log_{10}\frac{A}{T} \tag{4}$$

Substituting equation (3) into equation (4), approximating sin D by D, and replacing D with the epicentral distance R (km) leads to

$$I(R)=I_0+C_1+C_2(\gamma R\log_{10}\mathrm{e}+\log_{10}R) \tag{5}$$

where C_1 and C_2 are new constants, and $\mathrm{e}=2{\cdot}72$. Gupta and Nuttli[6] used $\gamma=0{\cdot}1$/deg in equation (5) for the eastern United States, and found $C_1=3{\cdot}7$ and $C_2=-2{\cdot}7$ for $R\geqslant 20$ km.

Equation (5) is a special form of equation (9) in Howell and Schultz.[8] Their paper emphasizes that the preceding argument is not unique, and that other forms of this attenuation function can be physically motivated. It was shown by Shebalin,[17] for example, that describing the attenuation of seismic energy by use of geometric spreading and inelastic attenuation leads to the general equation describing the macroseismic field

$$I(\Delta)=bM-v_0\log_{10}\Delta-p\Delta+C_0 \tag{6}$$

where M is earthquake magnitude, b, v_0, p and C_0 are constants and $\Delta=(R^2+H^2)^{1/2}$. M can be approximated by a linear function of maximum intensity (e.g. $M=1+\frac{2}{3}I_0$; Richter[16]). It is seen that equations (5) and (6) are of equivalent form. If the assumptions involved in the derivation of equation (5) are reasonable, then it should also apply to other parts of the world by using a value of γ appropriate to that region.

For regions 1 and 3 (Figure 1) and for the given maximum intensity I_0 the average and the standard deviation of $\log_{10}\Delta=\log_{10}(R^2+H^2)^{1/2}$ have been computed for each of the intensities I_1 and tabulated in Tables I(a) and I(b), when $I_1=I_0, I_0-1, I_0-2\ldots$. The average values of $\log_{10}\Delta$ were then fitted by eight different regression equations. Detailed analysis of these eight equations and considering seven ($b_1, b_2, \ldots, b_7$) regression coefficients[30] shows that the best choice for the empirical attenuation equation is

$$I_1-I_0=b_2+b_3\log_{10}\Delta+b_4\Delta/100 \tag{7}$$

with $b_2=3{\cdot}04\pm0{\cdot}87$, $b_3=-2{\cdot}64\pm0{\cdot}66$ and $b_4=-0{\cdot}98\pm0{\cdot}40$ in region 1 and $b_2=3{\cdot}55\pm0{\cdot}52$, $b_3=-3{\cdot}43\pm0{\cdot}41$ and $b_4=-0{\cdot}47\pm0{\cdot}27$ in region 3. This equation has been adopted for all subsequent analyses in this work. It is equivalent in form to equation (5) if Δ is taken to correspond to R and if $C_1=b_2$, $C_2=b_3$ and $\gamma=b_4/(100\,b_3\log_{10}e)$.

Gupta and Nuttli[6] used $\gamma=0{\cdot}1$/deg ($=0{\cdot}0009$/km) for eastern United States while Nuttli[15] used $\gamma=0{\cdot}60$/deg ($=0{\cdot}0054$/km) for California. It is interesting to compare these results with the possible interpretation of the regression results using equation (7). Assuming that some physical analogy can be drawn between equations (3) and (5) or (7) one can compute the values of γ implied by the coefficients b_3 and b_4 above. These results are summarized in Table II, and suggest comparable and larger γ than $\gamma=0{\cdot}005$/km for California in region 1. In region 3, γ takes on smaller values.

With a larger data base and with more detailed analyses of the validity of such inferences, it may become possible to associate the above variations in γ with the details of the tectonic regime in regions 1 and 3 of the Balkan peninsula. Having established better the underlying physical similarities of this area relative to the western United States, it may also become possible to use such inferences to justify the use of the data, recorded in the western United States, for engineering design in appropriate regions of the Balkan countries and *vice versa*.

Tables III(a) and III(b) present averages and standard deviations of the logarithm of the hypocentral distance to the isoseism enclosing $I\geqslant I_1$. These tables have been computed by using equation (7) and represent smooth surfaces through the available data represented by Tables I(a) and I(b).

In Figure 7, attenuation equations for regions 1 and 3 have been plotted on the same scale for $I_0=$ X and versus distance $\Delta=(R^2+H^2)^{1/2}$. For comparison, the average attenuation equations applicable to the western and central and eastern United States (assuming $H=0$) have been plotted also. It is seen that the overall slope of both attenuation equations is very similar to that in the western United States. Translation of these curves, relative to each other and relative to the western United States data, can be explained by the variation of the average focal depth of earthquakes in the respective regions. Region 3, for example, which has the 'lowest' attenuation curve in Figure 7, has many shallow sources, many less than 10 km, and most less than 20 km deep [Figure 5(b)].

Table II. Coefficient of 'anelastic attenuation γ' for different regions computed from $\gamma=b_4/(100b_3\log_{10}e)$

	b_3	γ
1	$-2{\cdot}64+/-0{\cdot}66$	0·0087
3	$-3{\cdot}43+/-0{\cdot}41$	0·0032

Table III. Computed average and standard deviation of the logarithm of the hypocentral distance in kilometers to isoseism enclosing the area with $I \geqslant I_1$

(a) REGION 1

EPICENTRAL INTENSITY, I_0	3	4	5	6	7	8	9	10
3·0	1·105 0·154							
4·0	1·431 0·160	1·105 0·154						
5·0	1·716 0·188	1·431 0·160	1·105 0·154					
6·0	1·954 0·151	1·716 0·188	1·431 0·160	1·105 0·154				
7·0	2·146 0·149	1·954 0·151	1·716 0·188	1·431 0·160	1·105 0·154			
8·0	2·302 0·145	2·146 0·149	1·954 0·151	1·716 0·188	1·431 0·160	1·105 0·154		
9·0	2·428 0·082	2·302 0·145	2·146 0·149	1·954 0·151	1·716 0·188	1·431 0·160	1·105 0·154	
10·0	2·533 0·162	2·428 0·082	2·302 0·145	2·146 0·149	1·954 0·151	1·716 0·188	1·431 0·160	1·105 0·154

(b) REGION 3

EPICENTRAL INTENSITY, I_0	3	4	5	6	7	8	9	10
3·0	1·019 0·182							
4·0	1·298 0·201	1·019 0·182						
5·0	1·566 0·209	1·298 0·201	1·019 0·182					
6·0	1·817 0·231	1·566 0·209	1·298 0·201	1·019 0·182				
7·0	2·045 0·198	1·817 0·231	1·566 0·209	1·298 0·201	1·019 0·182			
8·0	2·246 0·117	2·045 0·198	1·817 0·231	1·566 0·209	1·298 0·201	1·019 0·182		
9·0	2·418 0·036	2·246 0·117	2·045 0·198	1·817 0·231	1·566 0·209	1·298 0·201	1·019 0·182	
10·0	2·564 0·201	2·418 0·036	2·246 0·117	2·045 0·198	1·817 0·231	1·566 0·209	1·298 0·201	1·019 0·182

INTENSITY, I_1

DISCUSSION AND CONCLUSIONS

The quality of the estimates for the mean and standard deviations of the distances for a given isoseismal depend on the number of radii used in the analysis. About 100 radii, or contributions from at least 7 earthquakes are needed, assuming that each earthquake contributes up to 16 radii.[1] Consequently, those μ_{I_0,I_1}

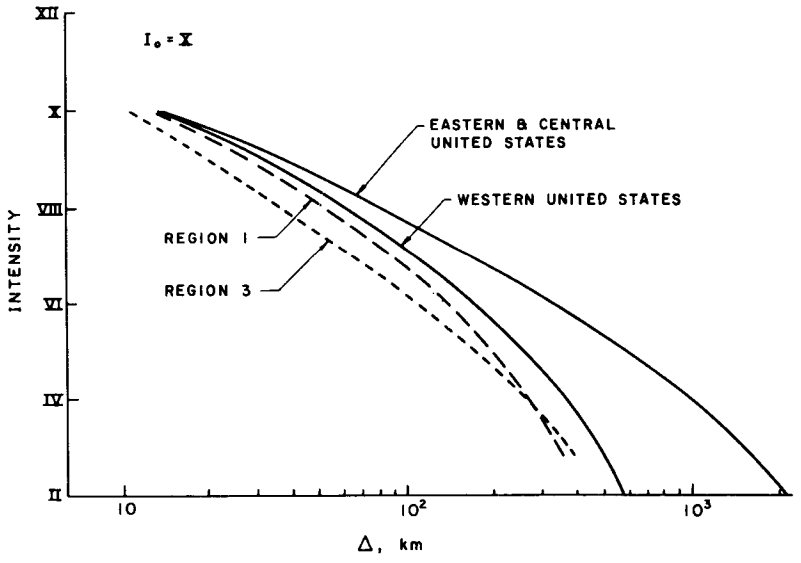

Figure 7. Comparison of the attenuation of MKS intensities with hypocentral distance in regions 1 and 3, for $I_0 = X$, with attenuation of MMI in the western and eastern United States (for $\Delta = R$, i.e. when H is not considered explicitly)

and σ_{I_0,I_1} which are determined by 100 or more radii to isoseism boundaries can be considered 'well-determined'. Perusal of Tables I(a) and I(b) will give the reader a detailed impression on how reliable and how many good estimates there are in the data, region by region.

For intensities III and smaller, the average radii to isoseism tend to increase more slowly, relative to the radii for intensities IV, than one would expect from the corresponding increases at the higher levels of intensity. Such trends were observed also in previous studies (e.g. Everenden *et al.*,[4] Anderson,[1] Gupta and Trifunac[5]) and suggest that these small intensities are at the threshold level of human perception, about 5–10 cm/sec^2 ground acceleration for intensity III.[24] Several average radii, μ_{I_0,I_1} in Tables I(a) and I(b) fall in this category and thus should be considered suspect and not representative of this data base. An obvious example of these for $I_1 = III$ is $\mu = 2{\cdot}149$ for $I_0 = VII–VIII$ (i.e. 7·5) in Table I(a). Other less obvious cases are undoubtedly present in the data base for $I_1 = III$.

Some uncertainties and scatter in the data occur because the epicentral intensity may not be determined with sufficient accuracy and because the discrete levels of the intensity scale, through discretization of the continuous physical process, inevitably increase the scatter of the overall data on the radii to I_1. The maps of all earthquakes considered in this study[19] have I_0 identified either by a discrete level, say X, or by the range, e.g. IX to X. To improve the situation somewhat, we have assigned numerical values corresponding to the Roman numerals of the MKS scale, $I_0 = 9{\cdot}5$ to an earthquake labelled by $I_0 = IX$ to X, for example. This reduces the discretization error slightly, but does not eliminate it. This, of course, assumes that the levels of the discrete descriptive scale can be assigned to the uniformly increasing numerical scale. Past analyses have shown that this convenient but not physical assumption is not seriously violated by the observed data and by other available inferences on the intensity scales.[20–22, 24] Assumptions of this type could be avoided by the use of indicator variables, but that would require a considerably larger data base than that available at present.

Another problem with estimation of intensities near the epicentre is that there is usually only a small number of independent estimates on the effects of shaking just above the earthquake. On the other hand, smaller intensities away from the epicentre cover larger areas, thus poducing more sampling points, and the contouring process tends to average out the uncertainties there. Thus, the quality and the realiability of μ_{I_0,I_1} and σ_{I_0,I_1} are low at or near I_0, then improve for intermediate distances, and again become worse as I_1 approaches the threshold level of perceptibility, at larger distances.

Previous studies by Anderson[1] and Gupta and Trifunac[5] used epicentral distance to analyse the distribution functions of the radii to isoseismals although it has been suggested that regional differences in the average depth of earthquakes[8] would suffice to explain the differences in the average attenuation rates for different geologic provinces. Thus, when the data on focal depths are available, inclusion of this information into the regression analyses of the distribution of the radii should reduce the scatter and the uncertainties in the results. We chose to take advantage of this approach in this investigation, by carrying out all the analyses described here in terms of $\Delta=(R^2+H^2)^{1/2}$ rather than R alone as in Anderson[1] and Gupta and Trifunac.[5] We chose this approach aware of the fact that many focal depths for the data in the final report on the Balkan project (Shebalin *et al.*[19]) have been determined in terms of the macroseismic data for the same earthquakes, and not by some other independent means.

Another factor which also influences the rate of attenuation of intensities with distance, and which interacts with the effects of the focal depth, is the size of the fault surface. This effect is particularly significant for shallow earthquakes and for the shape of attenuation with respect to R (or Δ) for the distribution of radii of I_0 and I_1 near I_0. The finite dimensions of the sources and its effects on the inferences about this data base were neither considered in the Balkan project (Shebalin *et al.*[19]), nor in this study.

As in Anderson,[1] the radii, R_i, in this work were measured from the geometrical centre of the isoseismal bounding the area assigned to I_0. In all instances the epicentral coordinates have been identified in this manner and not from some other independent or instrumental determination. Using the instrumentally determined epicentres, if those were available, would have increased the variation of the measured radii, because it is possible that for many (relatively larger) earthquakes the 'epicentre' of I_0 isoseismal does not coincide with the instrumentally determined epicentre.

Figure 7 suggests that the attenuation in Albania and Yugoslavia seems to be very similar to the attenuation of mean intensities in the western United States. Large standard deviations of all estimates in Tables I(a) and I(b) suggest that the method of analysis in this paper is not well suited to study the details of the differences in attenuation and to detect small differences which are clearly overshadowed by the large scatter in the data. In any case for the same average depth of foci one would not expect to see significant differences in the shapes of the average attenuation curves for $\Delta<100$ to 200 km, even if the respective geological environments were quite different. The distance range $0<\Delta<200$ km is of particular interest to earthquake engineering, because the damaging motions typically occur there, and because the calculations show that the contributions to seismic risk estimates are very significant within this distance range.[31]. Therefore, Figure 7 also suggests that the assumption that the attenuation of seismic intensity in Albania and Yugoslavia is similar to that in California (and the western United States) is not contradicted by the data which are considered in this work. This suggests that some other related characteristics of strong ground motion, for example, the relationship between the discrete levels of the intensity of shaking and of the characteristics of recorded strong ground motion, might be similar as well. Such assumptions must be carefully verified, before detailed seismic risk calculations can be carried out in Albania and Yugoslavia, using computer programs developed and 'calibrated' for the western United States. An indication that the physical characteristics of the two respective environments are not too dissimilar suggests better and simpler ways for careful calibration and translation of the experiences from one region with abundant data to another where the data are not adequate at present to arrive at independent estimates.

REFERENCES

1. J. G. Anderson, 'On attenuation of Modified Mercalli Intensity with distance in the United States', *Bull. seism. soc. Am.* **68**, 1147–1179 (1978).
2. J. G. Anderson and M. D. Trifunac, 'Uniform risk functionals for characterization of strong earthquake ground motion', *Department of Civil Engineering Report No. 77-02*, University of Southern California, Los Angeles, CA, 1977.
3. G. A. Bollinger, 'Reinterpretation of the intensity effects of the 1886 Charleston, South Carolina, earthquake, in 'Geological geophysical and seismological studies related to Charleston, South Carolina earthquake of 1886; a preliminary report' (Ed. D. W. Rankin), *U.S. Geological Survey Profess. Paper 1028*, 1977.
4. J. F. Everenden, R. R. Hibbard and J. S. Schneider, 'Interpretation of seismic intensity data', *Bull. seism. soc. Am.* **63**, 399–422 (1973).
5. I. D. Gupta and M. D. Trifunac, 'Attenuation of intensity with epicentral distance in India', *Int. j. soil dyn. earthquake eng.* **9**, 162–169 (1988).
6. I. N. Gupta and O. W. Nuttli, 'Spatial attenuation of intensities for central U.S. earthquakes', *Bull. seism. soc. Am.* **66**, 743–751 (1976).

7. P. G. Hoel, *Introduction to Mathematical Statistics*, Wiley, New York, 1971.
8. B. F. Howell and T. R. Schultz, 'Attenuation of Modified Mercalli Intensity with distance from the epicenter', *Bull. seism. soc. Am.* **65**, 651–665 (1975).
9. L. Jordanovski, V. W. Lee, M. Manić, T. Olumčeva, C. Sinadinovski, M. Todorovska and M. D. Trifunac, 'Strong earthquake ground motion data in Eqinfos: Yugoslavia, Part, I', *Department of Civil Engineering Report No. 87-05*, University of Southern California, Los Angeles, CA, 1987.
10. V. W. Lee, 'Seismic microzonation method based on Modified Mercalli Intensity scaling', *Earthquake eng. and eng. vib.*, **7**, No. 3, 47–63 (1987).
11. V. W. Lee and M. D. Trifunac, 'Uniform risk spectra of strong earthquake ground motion', *Department of Civil Engineering Report No. 85-05*, University of Southern California, Los Angeles, CA, 1985.
12. V. W. Lee and M. D. Trifunac, 'Microzonation of a metropolitan area', *Department of Civil Engineering Report No. 87-02*, University of Southern California, Los Angeles, CA, 1987.
13. O. W. Nuttli, 'The Mississippi Valley earthquakes of 1811 and 1812: Intensities, ground motions and magnitudes', *Bull. seism. soc. Am.* **63**, 227–248 (1973).
14. O. W. Nuttli, 'Seismic wave attenuation and magnitude relations for eastern North America', *J. geophys. res.* **78**, 876–885 (1973).
15. O. W. Nuttli, 'Comments on 'Seismic intensities, 'size' of earthquakes and related parameters' by Jack F. Everenden', *Bull. seism. soc. Am.*, **66**, 331–338 (1976).
16. C. F. Richter, *Elementary Seismology*, Freeman and Co., San Francisco, 1958.
17. N. V. Shebalin, 'Metody ispolzovaniya inzhenerno- seismologicheskikh dannykh pri seismicheskom rayonirovanni', *Seismicheskoye rayonirovaniye SSSR*, Nauka, 1968.
18. N. V. Shebalin, 'Makroseismicheskoye pole i ochag silnogo zemletryaseniya', *Dissertation*, Institute of the Physics of the Earth, Moscow, 1969.
19. N. V. Shebalin, V. Karnik and O. Hadžievski (Eds.), *Catalogue of Earthquakes (Part I, 1901–1970, Part II, prior to 1901)*, UNDP/UNESCO Survey of the Seismicity of the Balkan Region, UNESCO, Skopje, Yugoslavia, 1974.
20. M. D. Trifunac, 'A note on the range of peak amplitudes of recorded accelerations, velocities and displacements with respect to the Modified Mercalli Intensity', *Earthquake notes* **47**, No. 2, 9–24 (1976).
21. M. D. Trifunac, 'Response spectra of earthquake ground motion', *J. eng. mech. div. ASCE* **104**, 1081–1097 (1978).
22. M. D. Trifunac, 'Preliminary empirical model for scaling Fourier amplitude spectra of strong motion acceleration in terms of Modified Mercalli Intensity and geologic site conditions', *Earthquake eng. struct. dyn.* **7**, 63–74 (1979).
23. M. D. Trifunac, 'A microzonation method based on uniform risk spectra', *Int. j. soil dyn. earthquake eng.* (in press).
24. M. D. Trifunac and A. G. Brady, 'On the correlation of seismic intensity scales with the peaks of recorded strong ground motion', *Bull. seism. soc. Am.* **65**, 139–162 (1975).
25. M. D. Trifunac and V. W. Lee, 'Empirical models for scaling Fourier amplitude spectra of strong motion acceleration in terms of earthquake magnitude, source to station distance, site intensity and recording site conditions', *Int. j. soil Dyn. and earthquake eng.* (in press).
26. M. D. Trifunac and V. W. Lee, 'Empirical models for scaling pseudo relative velocity spectra of strong earthquake accelerations, in terms of magnitude, distance, site intensity and recording site conditions', *Int. j. soil dyn. earthquake eng.* (in press).
27. M. D. Trifunac and V. W. Lee, 'Direct empirical scaling of response spectral amplitudes for various site and earthquake parameters', *Report NUREG/CR-4903*, Vol. 1, U.S. Nuclear Regulatory Commision, 1987.
28. M. D. Trifunac, J. G. Anderson and V. W. Lee, 'Methods for introduction of geological data into characterization of active faults and seismicity and upgrading of the uniform risk spectrum technique', *Report NUREG/CR-4903*, Vol. 2, U.S. Nuclear Regulatory Commission 1987.
29. M. D. Trifunac, J. G. Anderson, B: D. Westermo and H. L. Wong, 'Methods for prediction of strong earthquake ground motion', *NUREG/CR-0689*, U.S. Nuclear Regulatory Commission, Washington, D.C., 1979.
30. M. D. Trifunac, V. W. Lee, H. Cao and M. I. Todorovska, 'Attenuation of seismic intensity in Balkan countries', *Department of Civil Engineering Report No. 88-01*, University of Southern California, Los Angeles, CA, 1988.
31. B. D. Westermo, M. D. Trifunac, J. G. Anderson and M. Dravinski, 'Seismic risk tables for pseudo relative velocity spectra in regions with shallow seismicity', *Department of Civil Engineering Report No. 80-01*, University of Southern California, Los Angeles, CA, 1980.